Damped Alfvén-Wave Transmission in Bismuth

D. J. BARTELINK AND W. A. NORDLAND
Bell Telephone Laboratories, Murray Hill, New Jersey
(Received 28 July 1966)

Measurements are reported on the transmission of transverse hydromagnetic waves in the low Mc/sec range through sizable samples of Bi at 4.2°K. The transmission is characteristic of the classical skin effect and has some of the well-known properties of the transverse magnetoresistance effect in Bi. The wave properties, moreover, give rise to a rotation of the axis of polarization at low magnetic field. Rotation can be a Faraday rotation resulting from residual Hall effect, or can be due to the anisotropy of the Bi Fermi surface. The experimental results are in qualitative agreement with an interpretation based on the latter effect.

I. INTRODUCTION

WE present herein experimental measurements of the low-frequency transmission of damped Alfvén waves in Bi at 4.2°K along a static applied magnetic field. The problem of damped Alfvén-wave transmission is just the classical skin-depth problem for a wave penetrating a conducting medium. When the incident wave consists of transverse fields, the skin depth depends on the resistivity at right angles to the direction of propagation. For such transverse waves directed along a magnetic field in Bi, as is the situation for the present experiment, this transverse resistivity is a strong function of the magnetic field. Bi has a large transverse magnetoresistance ratio because the compensation of carriers prevents the buildup of a Hall voltage and the carriers drift at the Hall angle relative to the electric field. The well-known properties of magnetoresistance are also evident in damped Alfvén waves. In addition, the wave nature of the disturbance gives rise also to the storage and transport of energy, so that, besides attenuation, there are the usual wave features of phase and polarization. It is the purpose of this paper to establish and compare with experiment the fundamental relations which govern the behavior of damped Alfvén-wave transmission. Presented also are experimental results on deviations from the relation which would occur in the simplest case. A qualitative interpretation in terms of a rotation of the axis of polarization is given.

In solid-state plasmas, hydromagnetic waves, such as helicon and Alfvén waves, are damped by carrier collisions. As is well known, helicon waves are a manifestation of the Hall effect in uncompensated materials and the amount of their damping is determined by the Hall angle. Alfvén waves in a compensated material such as Bi, which has little net Hall effect, depend instead upon the inertial effect of the carrier mass. In order for collision damping to be weak, not only must the Hall angles of the carriers be large, but the Alfvén-wave fields must fluctuate with a frequency greater than the carrier collision frequency. At low frequencies, where the present experiments are carried out, the Alfvén waves are heavily damped although the Hall angles of the individual carrier species are usually large.

Alfvén waves were first found to propagate in Bi by Buchsbaum and Galt[1] using microwave frequencies greater than the carrier-collision frequency at 4.2°K, so that damping was a small perturbation. Plasma properties measured by Alfvén-wave propagation in[2,3] Bi and other materials, such as[4] Sb and graphite,[5] have been deduced from the phase velocity of the wave. The Fermi surface of Bi has been probed in this way.[6–10]

Damped Alfvén waves at low radiofrequencies can be transmitted through sizable Bi samples because for magnetic fields of the order of 1 kG the skin depth equals 1 cm at 1 Mc/sec. An early report of this transmission has previously been given,[11] and similar physics was subsequently used to verify the Doppler interaction between transverse waves and a drift current applied parallel to the direction of wave propagation.[12] As expected, the axis of polarization was found to rotate in proportion to the current.

Damped Alfvén waves have been observed in materials other than Bi. For instance, transmission through Sb has been observed by the authors in unpublished work. Damped Alfvén waves, accompanied by rotation of the axis of polarization, may also be responsible for the observed results of Taylor, *et al.*[13] for Sn and Pb, as has been remarked by Grimes.[14] These latter are compensated materials which nevertheless showed experimental behavior resembling dimensional resonances of

[1] S. J. Buchsbaum and J. K. Galt, Phys. Fluids **4**, 1514 (1961).
[2] G. A. Williams, Bull. Am. Phys. Soc. **7**, 409 (1962); **8**, 205 (1963); Phys. Rev. **139**, A771 (1965).
[3] B. W. Faughnan, J. Phys. Soc. Japan **20**, 575 (1965).
[4] G. A. Williams, Bull. Am. Phys. Soc. **9**, 353 (1963).
[5] M. Surma, J. K. Furdyna, and H. C. Praddaude, Phys. Rev. Letters **13**, 710 (1964).
[6] J. Kirsch and P. B. Miller, Phys. Rev. Letters **9**, 421 (1962).
[7] J. Kirsch, Bull. Am. Phys. Soc. **8**, 205 (1963); Phys. Rev. **133**, A1390 (1964).
[8] M. S. Khaikin, V. S. Edel'man, and R. T. Mina, Zh. Eksperim. i Teor. Fiz. **44**, 2190 (1963) [English transl. Soviet Phys.—JETP **17**, 1470 (1963)].
[9] M. S. Khaikin, La Fal'kovskii, V. S. Edel'man, and R. T. Mina, Zh. Eksperim. i Teor. Fiz. **45**, 1839 (1963) [English transl. Soviet Phys.—JETP **18**, 1167 (1964)].
[10] G. A. Williams and G. E. Smith, IBM J. Res. Develop. **8**, 276 (1964).
[11] D. J. Bartelink, Bull. Am. Phys. Soc. **8**, 205 (1963).
[12] D. J. Bartelink, Phys. Rev. Letters **12**, 479 (1964).
[13] M. T. Taylor, J. R. Merrill, and R. Bowers, Phys. Rev. **129**, 2525 (1963).
[14] C. C. Grimes, G. Adams, and P. H. Schmidt, Phys. Rev. Letters **15**, 409 (1964).

helicons. Buchsbaum and Wolff[15] have shown that in materials with "open orbits" the damping of helicons can become quite pronounced for certain critical magnetic-field directions. The resulting wave propagation was found by Grimes[14] to have a behavior similar to damped Alfvén waves.

The penetration depth of damped Alfvén waves as determined from our experimental results is related to an average value of $\omega_c\tau$, in which $\omega_c\tau$ for each carrier species is weighted according to the relative concentration of the species (ω_c and $1/\tau$ are the cyclotron and collision frequencies, respectively). This average, which we denote as $\langle\omega_c\tau\rangle$, is also obtainable from magnetoresistance measurements and, as a result, damped Alfvén-wave measurements offer little advantage in determining τ for each species, particularly its anisotropy. They offer, however, a probeless method of measurement, and the measurement of the rotation of the axis of polarization is an additional piece of information.

Damped Alfvén-wave transmission is closely related to magnetoresistance, and a qualitative understanding of this relation can be obtained from a study of the five configurations shown in Fig. 1. Each diagram [(a) to (e)] represents a sample, typically Bi, in a magnetic field **H**. In (a) we show a method of measuring magnetoresistance between two points. The voltage V will be a strong function of **H** but it is generally a weak function of the frequency of the current I. In (b) the voltage is measured across contacts on the bottom face aligned in the field **H** with those on the top. At fields where the resistance along the field is negligible compared with that at right angles, the voltages in (a) and (b) will be equal for dc. In (c), there the contacts are rotated 90°, no voltage will be measured with dc. One might think of the distribution of electric field, **E**, in the sample as the field between two equipotential cylinders extending down from the current contacts.

Consider now ac measurements and recall that the skin depth in a conductor is inversely proportional to frequency. We expect the field **E** to decay with distance from the current terminals. The actual field amplitudes associated with the wave properties must be obtained from a solution of the wave equation, as is done, for example, in the next section. From a causality argument, however, it is plausible that **E** will have a phase lag with distance and that a characteristic wavelength is pertinent. The characteristic attenuation of the skin depth is associated with this phase lag because, unlike the dc case, the source current cannot maintain **E** deep in the bulk when the current and the **E** field are out of phase. Clearly the fields exist in the bulk only because of a directed energy flux or wave. Such waves can be launched and detected also by their magnetic field through an rf coil, as indicated in configurations (d) and

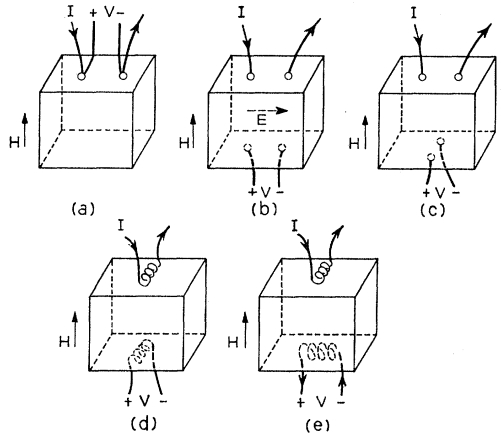

FIG. 1. Idealized configurations of Bi samples in a magnetic field which are used in the text to compare magnetoresistance and damped Alfvén-wave effects.

(e) of Fig. 1. These configurations are equivalent to (b) and (c), except for the advantage that coils can be made to rotate freely.

The polarization of the propagating wave may rotate about the vertical axis so that a nonzero voltage could be observed in (c). Rotation can be induced, for example, by a Hall effect. The Hall effect is characterized by a current and electric field in a plane normal to H with an angular separation equal to the Hall angle. A small Hall effect is expected for Bi at low magnetic fields where the difference in electron and hole mobility can influence the effective compensation of the plasma. The resulting rotation, which might be called a Faraday rotation, will be small and will not affect the attenuation. For a large Hall effect, however, we obtain a helicon wave. Its skin depth includes many wavelengths because the large Hall angle gives rise to a relatively small Joule heating current for a given magnitude of **E**, and the energy flux is dissipated only after a large number of wavelengths.

Another cause for rotation of the axis of polarization in Bi, follows from the fact that because of the highly anisotropic masses, the wave velocity is a strong function of the polarization direction. This fact, we shall show, is responsible for the rotation observed in our experiments.

In Sec. II we analyze the propagation and damping of Alfvén and helicon waves and the characteristics of damped Alfvén waves. Three measurable features of damped Alfvén waves—their amplitude, phase, and polarization—are discussed in Sec. III. There we consider the rotation of a linearly polarized source signal by the Hall effect and by crystal anisotropy. In the Appendix we compare the Hall effect rotation induced by unequal $\omega_c\tau$'s with that produced by a drift current. In Sec. IV we present the experimental methods and results which illustrate the basic damped Alfvén-wave characteristics. The rotation measurements and their qualitative interpretation are described in Sec. V.

[15] S. J. Buchsbaum and P. A. Wolff, Phys. Rev. Letters **15**, 406 (1964).

II. ALFVÉN- AND HELICON-WAVE DAMPING

The characteristics of wave propagation and damping are readily understood from the properties of the current generated by the electric field of the wave. The ac conductivity tensor, $\boldsymbol{\sigma}$, of a magnetized plasma characterizes the current density j according to $\mathbf{j}=\boldsymbol{\sigma}\cdot\mathbf{E}$, where for a plasma consisting only of holes[16]

$$\boldsymbol{\sigma}=\frac{e^2n/m}{(\nu+i\omega)^2+\omega_c^2}\begin{pmatrix}\nu+i\omega & \omega_c & 0\\ -\omega_c & \nu+i\omega & 0\\ 0 & 0 & \nu+i\omega+\dfrac{\omega_c^2}{\nu+i\omega}\end{pmatrix}, \quad (1)$$

where ν, ω, and ω_c are the collision, wave, and cyclotron frequencies, and where e, m, and n are the charge, mass, and density, respectively. Current flow at right angles to $\mathbf{H}$ ($\mathbf{H}$ is taken to lie along the z direction) is described by the upper left 2×2 portion of the tensor. We restrict our discussions to propagation along $\mathbf{H}$, so that for a transverse wave only these currents are of interest. We consider the limit of high magnetic field and/or low frequency such that $\omega_c\gg\omega$. The denominator of the term multiplying the tensor in Eq. (1) is real (1) when $\omega_c\gg\nu$ for any $\omega\ll\omega_c$ or (2) when $\omega\ll\nu$ for any $\omega_c\gg\omega$. The diagonal elements of the 2×2 portion then consist of a pure real term (ν) and a pure imaginary term ($i\omega$). Since the diagonal terms describe current flow parallel to the driving electric field, the real term corresponds to an Ohmic current and thus describes the Joule heating which is done at the expense of the wave. The imaginary term, which corresponds to a 90° phase shift, produces a reactive current. When only a reactive current flows, an electric field can be induced in the conductor without Ohmic losses and the energy stored in the fields of the wave will not be dissipated. The phase shift is caused by the time lag of the response of particles with mass m to the time varying field.

Waves propagating (transmitting energy) on the basis of this energy storage mechanism, which are known as Alfvén waves, can occur in plasmas with equal densities of electrons and holes so that the off-diagonal term (ω_c) sums to zero. Alfvén waves have a mass-dependent phase velocity. When $\omega\ll\nu$ these waves are strongly collisionally damped because the induced current is largely dissipative. For $\omega\ll\nu$, $\boldsymbol{\sigma}$ reduces to the dc conductivity tensor (neglecting variations of ν with ω). The latter describes, in Bi, the transverse magnetoresistance effect inherent in the ω_c^2 term of the denominator of the leading term. This same effect governs much of the behavior of damped Alfvén waves.

In an uncompensated plasma the Hall angle is large when $\omega_c\gg\nu$ and the current induced by $\mathbf{E}$ flows at the Hall angle relative to it [see Eq. (1)]. Helicon waves propagate by means of the energy stored in the fields, which can exist without appreciable Ohmic losses under these circumstances. Helicon waves are circularly polarized, and their axis of polarization rotates through 2π in one wavelength. In Bi, for which the off-diagonal or Hall terms (ω_c) tend to cancel so that no helicon waves occur, a small amount of rotation may result from a small residual Hall term. The Bi plasma consists of electrons and holes in equal concentrations and their Hall terms, which are almost equal in magnitude, subtract. They do not cancel exactly when the electron and hole collision frequencies are comparable to the ω_c's, but the $\omega_c\tau$'s are different from each other.

Because of the presence of the electrons in three separate ellispoids as well as holes, we add a subscript s for each species to the parameters of Eq. (1) and obtain the total conductivity

$$\boldsymbol{\sigma}=\sum_s \boldsymbol{\sigma}_s. \quad (2)$$

The characteristics of Alfvén- and helicon-wave propagation and damping are included in Eq. (2). Wave solutions to Maxwell's equations, which describe these plasma properties, are obtained from the wave equation with a tensor dielectric constant $\boldsymbol{\epsilon}$, where in mks units

$$\boldsymbol{\epsilon}=\epsilon_l\mathbf{1}+\frac{\boldsymbol{\sigma}}{i\omega\epsilon_0}. \quad (3)$$

We assume that ϵ_l, which is the lattice dielectric constant, is negligibly small in all cases we are to consider. Clearly an imaginary term on the diagonal of $\boldsymbol{\sigma}$, such as the $i\omega$ term which yields the Alfvén wave, corresponds to a real term in $\boldsymbol{\epsilon}$. When such a real term is positive, the wave equation has wave solutions, which we take to be of the form $\exp[i(\omega t-kz)]$. Although $\boldsymbol{\sigma}$ is a tensor, it can be rewritten as a complex scalar quantity by the choice of a frame of reference rotating about $\mathbf{H}$. The resulting imaginary terms of σ are positive or negative depending on the sense of rotation. The corresponding dielectric constant has two values $\epsilon_\pm$ which depend on the choice of sense of circular polarization [$\epsilon_\pm=\epsilon_{xx}\pm i\epsilon_{xy}$, where ϵ_{xx} and ϵ_{xy} are elements of $\boldsymbol{\epsilon}$ computed from Eqs. (1) to (3)]. Using the foregoing equations we find the standard expression

$$\epsilon_\pm=\sum_s \frac{\omega_{ps}^2}{\omega(\pm\omega_{cs}-\omega+i\nu_s)}, \quad (4)$$

where $\omega_{ps}=(n_se_s^2/m_s\epsilon_0)^{1/2}$ is the plasma frequency. Multiplying each term in the sum top and bottom by $(\pm\omega_{cs}+\omega-i\nu_s)/\omega_{cs}$, we obtain $\epsilon_\pm$ in a form in which each term of Eq. (4) is itself the sum of three terms. These are recognizable as the same three terms as those of the tensor of Eq. (1), namely ω_c, $i\omega$, and ν,

[16] See, for example, W. P. Allis, S. J. Buchsbaum, and A. Bers, *Waves in Anisotropic Plasmas* (M.I.T. Press, Cambridge, Massachusetts, 1963), p. 19. For a convenient derivation of the dc conductivity tensor see C. Kittel, *Quantum Theory of Solids* (John Wiley & Sons, Inc., New York, 1963), p. 240.

respectively;

$$\epsilon_{\pm}=\frac{c^2}{\omega^2}\sum_s \omega e_s n_s\left(\pm 1+\frac{\omega}{\omega_{cs}}-\frac{i}{\omega_{cs}\tau_s}\right)\Big/ H(1+W_s) \quad (5)$$

where $\tau_s=1/\nu_s$ and

$$W_s=\frac{1}{(\omega_{cs}\tau_s)^2}-\frac{\omega^2}{\omega_{cs}^2}+\frac{2i\omega}{\omega_{cs}^2\tau_s}.$$

Since we have already assumed $\omega/\omega_{cs}\ll 1$, we can neglect the small imaginary term in W_s compared with unity unless $\omega_{cs}\tau_s$ is very small. It is usually sufficient to write

$$1+W_s=1+1/(\omega_{cs}\tau_s)^2. \quad (6)$$

The solutions to the wave equation, in general, give the wave number $k_{\pm}$ for the two polarizations according to

$$k_{\pm}^2=(\omega^2/c^2)\epsilon_{\pm}. \quad (7)$$

Hence

$$k_{\pm}^2=\frac{\omega en}{H}\left(\pm\frac{\delta n}{n}+\frac{\omega}{\langle\omega_c\rangle}-\frac{i}{\langle\omega_c\tau\rangle}\right), \quad (8)$$

where

$$\delta n/n=(en)^{-1}\sum_s e_s n_s/(1+W_c), \quad (9)$$

$$\langle\omega_c\rangle^{-1}=(n^{-1})\sum_s n_s/\omega_{cs}(1+W_s), \quad (10)$$

$$\langle\omega_c\tau\rangle^{-1}=(n^{-1})\sum_s n_s/\omega_{cs}\tau_s(1+W_s), \quad (11)$$

$$n=\sum_s n_s;\quad e=|e_s|.$$

The first term in Eq. (8), which is the Hall or helicon term, is, in the limit $W_s=0$, just proportional to the net charge density. For $W_s\neq 0$, it represents the effective net charge density which, as noted earlier, may be nonzero even though the electron and hole concentrations are unequal. The $\pm$ sign shows that it has different effect on the two senses of polarization. Equations (10) and (11) contain only sums over positive quantities.

The characteristic helicon dispersion relation is obtained when the $\omega/\langle\omega_c\rangle$ term can be neglected and $\langle\omega_c\tau\rangle\delta n/n\gg 1$:

$$k_{+}\cong\frac{\omega}{V_h}\left(1-\frac{in}{2\delta n\langle\omega_c\tau\rangle}\right), \quad (12)$$

where $V_h^2=\omega H/e\delta n$. One obtains the Alfvén wave when instead the $\delta n/n$ term is negligible and $\omega\langle\omega_c\tau\rangle/\langle\omega_c\rangle\gg 1$:

$$k_{\pm}\cong\frac{\omega}{V_A}\left(1-\frac{i}{2\omega\langle\tau\rangle}\right), \quad (13)$$

where $V_A^2=\langle\omega_c\rangle H/en$ and $\langle\tau\rangle=\langle\omega_c\tau\rangle/\langle\omega_c\rangle$. Damped Alfvén waves occur when both real terms in Eq. (8) are negligible compared with the third term (i.e., $\delta n\sim 0$; $\omega\langle\tau\rangle\ll 1$):

$$k_{\pm}=(\omega en/H)^{1/2}(1-i)/(2\langle\omega_c\tau\rangle)^{1/2}. \quad (14)$$

The attenuation per wavelength of Alfvén and helicon waves, i.e., $\mathrm{Im}k/\mathrm{Re}k$, clearly reduces as τ is increased. The attenuation per wavelength for damped Alfvén waves, on the other hand, is a constant factor $e^{-2\pi}$. The relative magnitude of the penetration depth of each of the three modes, however, is determined by a comparison of the attenuation coefficients $\alpha=\mathrm{Im}k$. The compensated plasma required for Alfvén waves can be compared with the helicon-wave plasma if we assume for the latter that $\delta n=n$, which corresponds to an uncompensated plasma with a concentration equal to the total concentration of the former. Hence, for damped Alfvén waves

$$\alpha_{dA}=-(\omega en/H)^{1/2}/(2\langle\omega_c\tau\rangle)^{1/2}$$

while for Alfvén and helicon waves, $\alpha_A=\alpha_{dA}/(2\omega\langle\tau\rangle)^{1/2}$ and $\alpha_h=\alpha_{dA}/(2\langle\omega_c\tau\rangle)^{1/2}$, respectively. A comparison of α_h and α_{dA} shows a result which is of use in establishing the ease of experimental detection of damped Alfvén waves, namely the following. We note first that the amplitude of a damped Alfvén wave and a helicon transmitted through a given thickness of comparable plasma (as defined above) will differ according to the magnitudes of the α's. Now if $\langle\omega_c\tau\rangle$ exceeds unity by only a small factor, e.g., <10, as is typical of many experiments, the amplitudes of the two transmitted signals can be made equal (i.e., $\alpha_H=\alpha_{dA}$) if the damped Alfvén wave is transmitted with a frequency lower than that of the helicon by only $2\langle\omega_c\tau\rangle$. This result illustrates the fact that, while the attenuation per wavelength of damped Alfvén waves is greater than that of the others, the measurable penetration is in many cases not drastically different. Thus, low-frequency wave transmission in a compensated plasma is not greatly more difficult than helicon transmission in a comparable uncompensated plasma. The strong damping per wavelength, however, makes the magnitude of the wavelength relatively unimportant in an experiment because, unlike the dimensional resonances of helicons, damped Alfvén waves are transmitted (as we shall see later) almost totally without influence of the boundaries of the sample. Of course many of the interesting properties of helicons are associated with the fact that transmission over many wavelengths takes place. Many of these effects do not occur for damped Alfvén waves.

III. DAMPED ALFVÉN-WAVE AMPLITUDE, PHASE, AND POLARIZATION

Two of the measurable properties of a wave, its amplitude and its phase, are directly related to the attenuation coefficient α and the propagation constant β, respectively. The third, its polarization, will be of concern to us later in the present section. The ratio, A, of the output amplitude to the input amplitude of a wave traveling over a distance z_0 in the z direction is related to α by

$$\ln A=\alpha z_0. \quad (15)$$

The phase delay, φ, of a wave directed along z is given in terms of β by

$$\varphi \equiv \omega \Delta t = \beta z_0, \tag{16}$$

where Δt is the time taken by a given reference phase of the wave to travel the distance z_0. Combining Eqs. (14), (15), and (16) we find for damped Alfvén waves

$$-\ln A = \varphi = z_0 \left(\frac{\omega e n}{2H \langle \omega_c \tau \rangle} \right)^{1/2}$$

$$\equiv z_0 \left(\frac{\omega}{2H} \sum_s \frac{e_s n_s}{\omega_{cs} \tau_s (1+W_s)} \right)^{1/2}. \tag{17}$$

The quantities $(\ln A)^2$ and φ^2 are proportional to $\mathrm{Im} k^2 [= (\omega^2/c^2)\ \mathrm{Im}\epsilon]$ so that by virtue of Eq. (3) they are proportional also to $\mathrm{Re}\sigma$. Their properties therefore include those of the dc magnetoconductivity, such as, for instance, the characteristic $1/H^2$ dependence of the conductivity associated with the transverse magnetoresistance of Bi. The major difference results from the frequency dependence introduced by the constant of proportionality of $\mathrm{Im}\epsilon$ and $\mathrm{Re}\sigma$[Eq. (3)]. A plot of the $\omega^{1/2}/H$ dependence of $\ln A$ and φ predicted by Eq. (17) in the limit that $W_s \to 0$ is shown in Fig. 2(a). At low magnetic fields, where $W_s \gg 1$, $\ln A$, and φ become independent of H. When the $\omega_{cs}\tau$'s of the various carrier species are widely different, in which case rotation effects might be expected, the $\ln A$ and φ curves can become more complicated [shown schematically in Fig. 2(b)], aside from any effects due to the polarization. Near the value of H for which the species (a) with the lowest $\omega_c\tau$ has $\omega_{ca}\tau_a \sim 1$ (i.e., $H = H_a$), the sum in Eq. (17) consists largely of the one term. In the limit of extreme differences in $\omega_c\tau$'s, the curve will have the steplike shape shown. The carrier species with the lowest value of $\omega_c\tau$ can, therefore, influence the shape of the curve provided this value is much lower than that of the others.

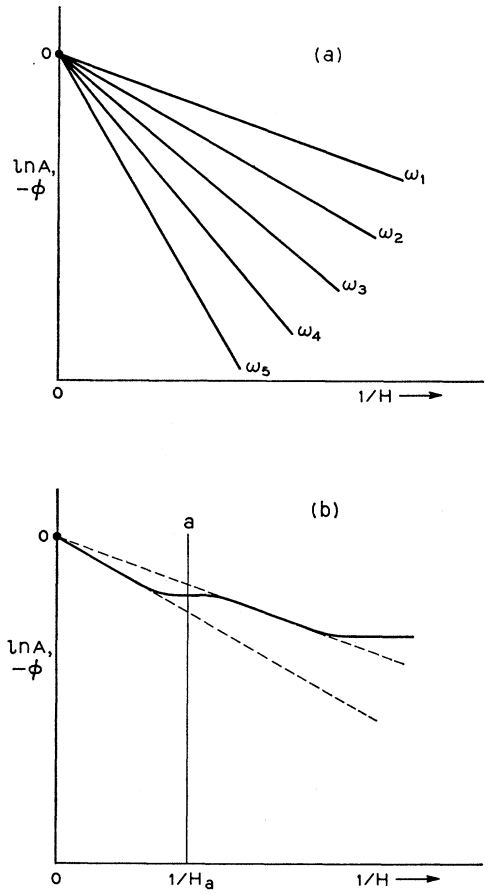

FIG. 2. (a) A plot of $\ln A$ or $-\varphi$ against $1/H$ yields a straight line in the high-field limit. The negative slope increases as $\sqrt{\omega}$, and the $H = \infty$ intercept corresponds to zero attenuation or phase delay. (b) Deviations from the linear slope, which occur at low field near $\omega_{ca}\tau_a = 1$, are shown schematically.

The rotation of the polarization axis of a linearly polarized input signal as a function of z can be analyzed in two ways. (1) The linear input can be resolved into two circularly polarized waves, each with its own characteristic velocity and attenuation, and these can be combined to give the resultant polarization. (2) It can also be resolved into two linearly polarized waves, polarized along two prefered (orthogonal) directions, each having separate properties, and then be reconstructed. Whichever analysis is used depends on which form of polarization provides the simplest analysis. The Hall effect rotation is easily analyzed in terms of circularly polarized waves, while the crystal anisotropy, which we feel is responsible for our observed results, is described more easily using linearly polarized waves.

Rotation is produced when the $\pm \delta n/n$ Hall effect term is nonzero, because the two circularly polarized components $\pm$ are transmitted with unequal wave numbers, i.e., $k_+ \neq k_-$. As one might expect, and as we show in the Appendix, the effect of this rotation on damped Alfvén waves is to change a linearly polarized input to an elliptically polarized wave. One reason for eliminating the Hall effect rotation as a possible explanation of our observed results is this elliptical polarization of the rotated wave. In some experimental cases, a rotated wave is observed which is still linearly polarized. Rotation of damped Alfvén waves without change to circular polarization occurs, however, when it results from a Hall effect induced by a drift current.[12] The two cases are compared in the Appendix where an analysis to lowest order is made of the effect of a small Hall term.

The anisotropy of the crystals has not been included in the analysis presented. We have tacitly assumed that the plasma was rotationally symmetric about **H**. For helicon waves, which have fields rotating about **H**, no change in the propagation characteristics is expected in anisotropic crystals when the crystal is physically rotated about **H** with respect to the source. (We ignore here such practical problems as coupling efficiency.)

Propagating Alfvén waves differ in this respect because, when linearly polarized, their fields interact with carriers such that only one mass component, averaged over a cyclotron orbit, determines the characteristics of the wave. Rotation of the crystal about **H** with respect to the source may, therefore, vary this component and with it the wave's propagation and damping characteristics. The velocity of Alfvén waves has been observed to vary significantly depending on its polarization,[2,3] and we expect damped Alfvén waves to be affected similarly.

The principal axes of the crystal offer the logical frame of reference in which to describe the behavior of the wave. When an incident wave of arbitrary linear polarization is resolved into components along these axes, therefore, a difference in their velocity will cause their reconstruction to yield a rotation of the axis of polarization. When the components consist of damped Alfvén waves, it is clear that, in general, an elliptically polarized wave will result, but that for a few specifically chosen situations a rotated linearly polarized wave could result. This effect in Bi is expected to be most pronounced for wave propagation along the bisectrix direction because there the Alfvén velocity has been found to depend most strongly on the direction of polarization.[2,3] A graphic illustration of the polarization dependence of V_A has been given by Buchsbaum.[17] We shall discuss the effect of the polarization dependence of damped Alfvén waves in the qualitative interpretation of the experimental results.

IV. OBSERVATION OF DAMPED ALFVÉN-WAVE TRANSMISSION

Damped Alfvén-wave transmission was observed at 4.2°K in Bi samples with the variety of configurations shown in Fig. 3. The single crystal material, which has a conductivity ratio (room temperature to 4.2°K) of up to 400, was grown by the method of quick freezing in a supercooled melt. The rf signals were launched and detected either electrically by probes and coupling transformers or magnetically by coils. The transformers consisted of a single-turn copper-foil primary on the sample side with a secondary of about 200 turns. Since transverse hydromagnetic waves are mainly a magnetic disturbance, coupling to them by coils is usually easier. The rapid attenuation of damped Alfvén wave coupled with the usual inefficiency in exciting waves in solid-state plasmas, however, necessitates good shielding between source and detector in order to observe the details of the transmission. Such shielding was readily achieved for all configurations of Fig. 3 except geometry (d), which used coils for both source and detector. The external shielding it required was obtained by the Bi enclosures shown as shaded areas.[18]

All data presented in this paper were taken with the magnetic field parallel to the direction of transmission, although qualitatively similar results have been observed with transverse fields. Reproducible results were obtained for each of the sample configurations and only the crystal orientation and sample temperature and quality influenced the results. Variation of the cross-sectional size or configuration resulted in no noticeable effects except in the magnitude of the response. We qualitatively understand this lack of dependence from the following considerations. The amplitude of transmission between a source and detector imbedded in an infinite medium depends on the solid angle formed by each at the location of the other, i.e., their transverse extent and their separation. In a waveguide, this angle and thereby the amplitude is increased by (we assume lossless) reflections from the boundaries, but the path length traveled is also increased. Normally, the phase delay produced by this longer path gives rise to interference effects which determine the mode of propagation. When the waves damp to a factor $e^{-2\pi}$ in one wavelength, however, these interference effects are not important. Most of the received signal will have traveled in a straight line, and the transverse size of the source

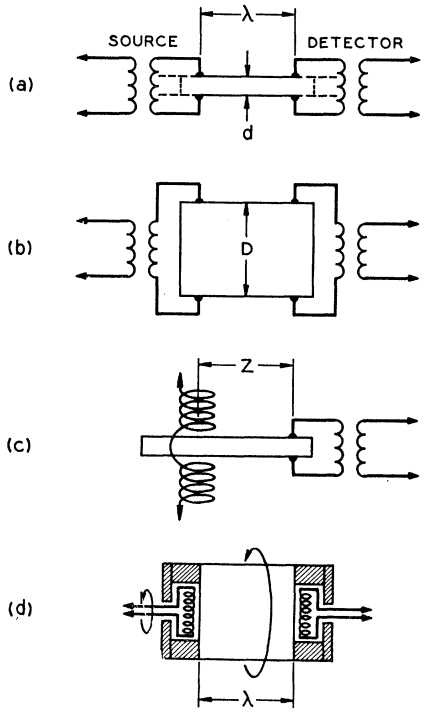

FIG. 3. Schematic representations of various sample configurations used to launch and detect damped Alfvén waves. In (a) and (b) transformers are used to couple to the electric field in samples of various size. Coils to couple to the magnetic field are used in (c) and (d) to obtain translation or rotation.

[17] S. J. Buchsbaum, in *Proceedings of the Symposium on Plasma Effects in Solids, Paris, 1964*, edited by J. Bok (Academic Press Inc., New York, 1965).

[18] Bi was used in order to match the thermal-expansion coefficient of the sample.

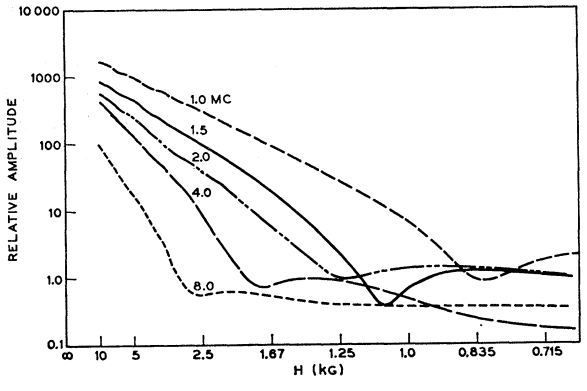

FIG. 4. Measured magnetic-field dependence of the amplitude ($\ln A$) of a signal transmitted over a 1-cm distance along the bisectrix direction at various frequencies.

and detector is more important than that of the waveguide. We have found in our experiments, that, when the source and detector are comparable in size with the distance between them, the characteristics of the transmission are influenced by geometry when the wavelength becomes long (damping low). When this effect occurs, it is seen on a plot of $\ln A$ vs $1/H$, which, instead of giving the predicted linear relation [see Fig. 2(a)], saturates or even turns down at large H. The relation between φ and $1/H$ remains very nearly linear in this case. Decreasing the source and detector size or increasing the sample length eliminates the saturation.

Measurements of the transmission of damped Alfvén waves were made in the following way. The amplitude or phase of the detector signal was plotted on the vertical axis of an X-Y recorder using, respectively, a logarithmic amplifier or a phasemeter. The reciprocal of the field was plotted directly using a modification of the recorder servosystem. Figure 4 shows typical results of amplitude as a function of field for transmission over a distance of 1 cm along the bisectrix direction. The cross-sectional dimensions of the sample, which had the configuration of Fig. 3(b), were 1×1 cm. A good linear dependence was observed for the curves of each of the various frequencies, except for a dip at low fields, which in the next section is related to rotation effects. The ratio of the slopes as $\sqrt{\omega}$ is within 7%. The value of $\langle\omega_c\tau\rangle$ can be determined from these slopes using Eq. (17). By assuming that for Bi $n\cong 6\times 10^{17}$ cm^{-3} and by using the average of the slopes in Fig. 4, we find that the magnetic field at which $\langle\omega_c\tau\rangle=1$ was 100 G, a value which is quite reasonable for this quality of material.

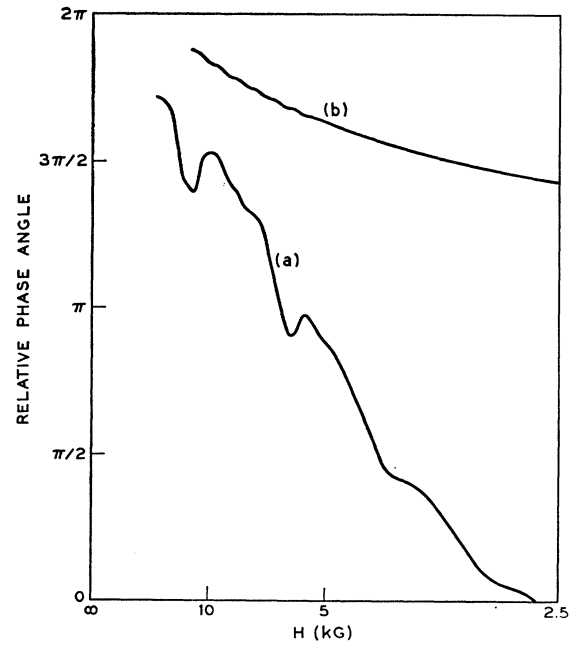

FIG. 5. Measured phase (φ) variation with field for transmission along the bisectrix, curve (a), and threefold, curve (b).

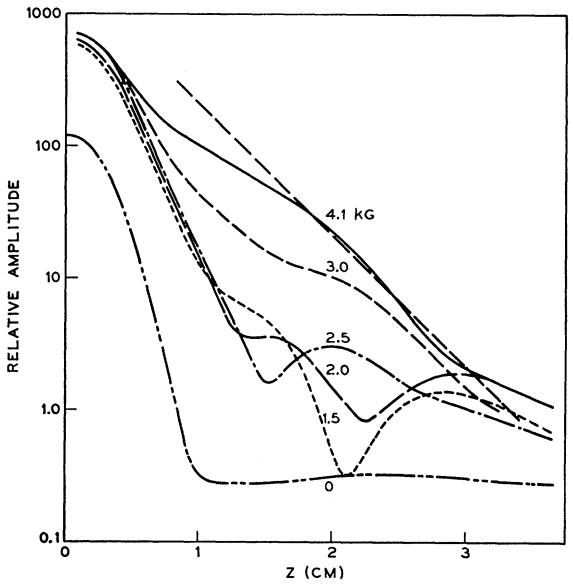

FIG. 6. Measured transmission amplitude variation with position of coils of the configuration of Fig. 3(c) for various values of magnetic field. The actual source position (near $z=0$) is somewhat uncertain.

The results of a high-field phase measurement for the bisectrix and threefold orientations are shown in Fig. 5(a) and 5(b), respectively. The Shubnikov–de Haas oscillations familiar in magnetoresistance measurements are seen here superimposed on a nearly linear relation between φ and $1/H$. The deviation of (b) from linearity is thought to arise from effects related to those sketched in Fig. 2(b).

The variation of $\ln A$ with length "z_0" of the transmission path along the bisectrix direction was measured at 2 Mc/sec using the geometry of Fig. 3(c). The resulting amplitude, shown in Fig. 6, exhibits an exponential decay which is modified by large quasioscillatory variations arising, we think, from rotation of the axis of polarization. The zero magnetic-field curve gives a

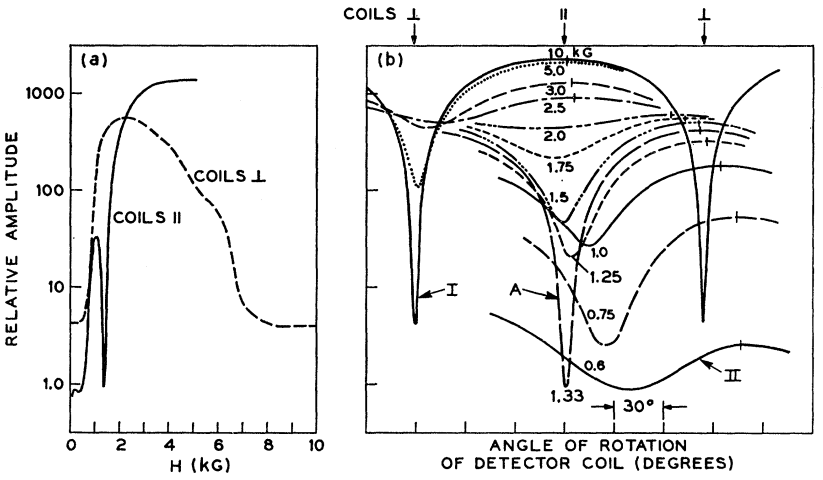

FIG. 7. (a) Amplitude vs field for the sample configuration of Fig. 3(d) with the coils parallel and orthogonal. The angle of the coils relative to the crystallographic directions is discussed in the text. (b) Amplitude response of detector coil vs coil angle for various magnetic-field values. Rotation of the axis of polarization and various degrees of elliptical polarization are evident.

measure of the signal leakage around the sample. The slope of $\ln A$ vs z for 4.1 kG, calculated from the value of $\langle\omega_c\tau\rangle$ determined previously, is shown by the dashed line.

V. AMPLITUDE DIP AT LOW MAGNETIC FIELD

The detailed behavior of the amplitude dip shown in Fig. 4 was investigated using 1 cm long samples with the configuration of Fig. 3(d). Circular and square cross-section samples were used but no difference was detected. The sample and one of the two coils could independently be rotated with respect to the other coil. The data shown in Figs. 7 to 9 are the amplitudes of transmission along the bisectrix direction obtained when the axes of the coils (rf magnetic field direction) were oriented along various transverse crystallographic directions. The sharpness of the amplitude dip was maximized by critical adjustment of the angle of the sample and coil, and for a critical value of the applied field the dip became a zero in response. The phase of the signal also experienced a rapid 180° reversal. Sharp dips have only been observed for transmission along the bisectrix axis. Along the binary axis the amplitude dependence on transverse orientation was small, while none was observed for the threefold axis.

The voltage generated in a solenoidal pickup coil, which is rotated with respect to a linearly polarized signal, has the angular dependence of a figure 8 pattern. A sharp minimum in coil voltage occurs only when the signal is linearly polarized; the angular variation resulting from an elliptically polarized wave has only a shallow minimum. Rotation of the axis of polarization of a linearly polarized signal launched by one coil will, therefore, give rise to a sharp null in the voltage across

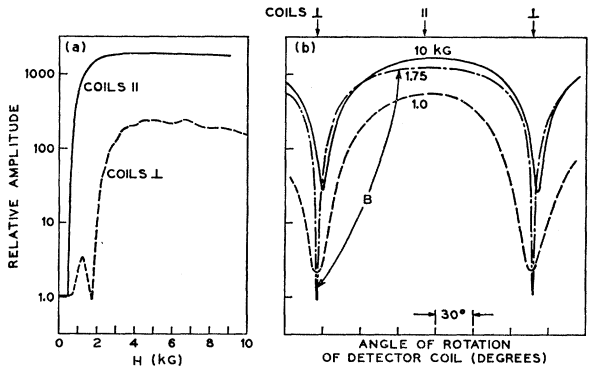

FIG. 8. Same as Fig. 7 except that the axis of the fixed coil was adjusted to give the sharp dip at low fields when the coils are perpendicular instead of parallel, as in Fig. 7.

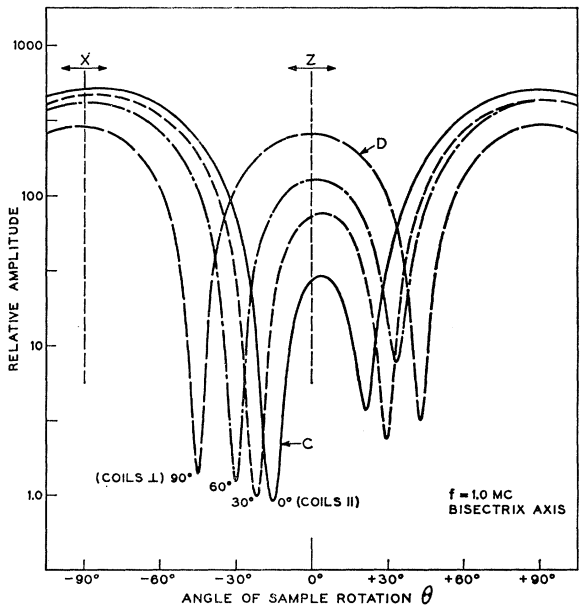

FIG. 9. Transmission amplitude as a function of sample angle Θ as the sample was rotated between the coils. The magnetic field was incrementally adjusted to give a sharp dip for each value of the angle between the coils, which is the parameter.

a parallel coil near the opposite face of a sample only when the angle of rotation is 90° and the signal is still linearly polarized. If the amount of rotation of the linearly polarized damped Alfvén waves were to be an increasing function of $1/H$, a response like that of Fig. 4 would occur. Measurements of the response with the coils parallel to each other, using the geometry of Fig. 3(d), as shown in Fig. 7(a) on a linear scale in H, showed the dip to be very sharp. The response obtained with the coils in quadrature had the expected broad maximum [Fig. 7(a) "coils $\perp$"].

An interpretation in terms of the Hall effect rotation of a linearly polarized wave, however, does not explain these results because this rotation is, as we have seen, of necessity accompanied by a change to elliptical polarization. The sharp dip shown in Fig. 7(a) cannot have been produced by an elliptically polarized wave. More detailed measurements, nevertheless, indicate that the transmission has the characteristics of a rotation, at least under certain conditions. These measurements were made by holding the sample angle fixed relative to the stationary coil at angle Ψ and recording the value of $\ln A$ as a function of the angle of the movable coil. Ψ is the angle between one of the crystallographic directions and the axis of the fixed coil.

The results, plotted in Fig. 7(b) for a particular value of Ψ, show that at high fields, e.g., 10 kG (curve I), a null was observable only with the two coils perpendicular, indicative of zero rotation. As the field was reduced, the minimum, which then occurred for different angles between the coils, shifted by an angular variation exceeding 90° at 0.6 kG (curve II). Superimposed on this change in angular position was a change in depth of the minimum. A very pronounced dip occurred at 1.33 kG (curve A), with the coils parallel. This dip, which was the same as that of Fig. 7(a), occurred with coils parallel for only one value of Ψ. For other values of Ψ a sharp dip was also observable, but with a different angle between the coils and sometimes a slightly different value of field. The data in Fig. 8 were taken with Ψ adjusted to give the sharp dip with the coils perpendicular. No rotation was observed.

Experimentally the only difference between the measurements of Figs. 7 and 8 was in the angle Ψ. This dependence on the transverse orientation of the crystal further rules out any interpretation in terms of the Hall effect rotation as defined in Sec. III because such effects are invariant with rotation of the crystal about the magnetic-field direction.

A more easily interpretable presentation of the low-field measurements was obtained by rotating the sample while holding the coils fixed relative to each other. In Fig. 9, which shows the result of this measurement for four different values of the angle between the coils, the magnetic-field strength was in each case just that required to produce the sharpest dip. The angular position of the crystal was recorded by a voltage proportional to Θ, which was taken as the angle between one of the

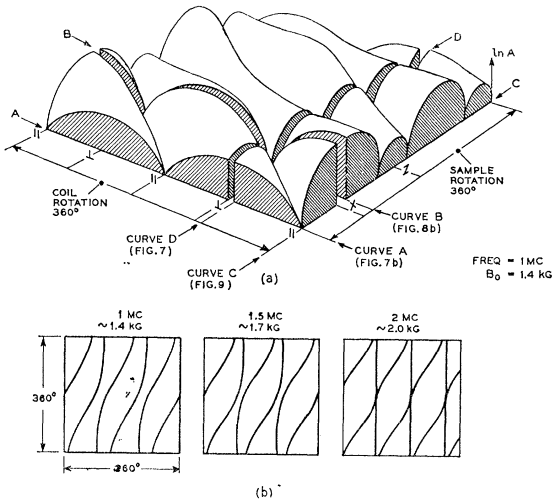

FIG. 10. (a) Schematic representation of the transmission amplitude ($\ln A$) as a function of coil rotation and sample rotation. The four intersecting planes labeled Curves A to D correspond to these curves in Figs. 7 to 9. (b) Plan view of (a) for various frequencies.

crystallographic directions (threefold) and the bisector of the angle between the coils. Thus, for example, with the coils parallel, the response at $\Theta=0$ and $\pm 90°$ (see curve C), is proportional to the attenuation of the amplitude of the rf magnetic field along the threefold and binary axes, respectively. It is seen from Fig. 9 that the responses at $\Theta=0°$ and 90° differ and that, when the coils are perpendicular, the amplitudes of the maxima become equal and the dip falls halfway between. Both conditions are expected from the symmetry of the configuration.

We have presented in Figs. 7, 8, and 9 four curves taken at the critical magnetic-field strength (~1.4 kG). These data contain the sharpest minima observed and are part of a relation of sharp minima in $\ln A$ as a function of coil and sample angle. This relation is shown schematically in Fig. 10(a). Curves A to D in Fig. 7, 8, and 9 represent extremal conditions in the plot of Fig. 10(a).

The three diagrams in Fig. 10(b) are schematic plan views of the $\ln A$ minima of Fig. 10(a) for three frequencies: the frequency of Fig. 10(a) and two others. The magnetic field at which the minima occurred was found to increase as the square root of the frequency, as is illustrated also by the dips in Fig. 4. This dependence strongly suggests that the occurrence of the minima is related to the wavelength [see Eq. (17)], a conclusion which is also supported by the spatial dependence of $\ln A$ shown in Fig. 6. The 2-Mc/sec diagram in Fig. 10(b) shows that two minima coalesce at that frequency with both coils parallel to the threefold axis. In the neighborhood of this point, rapid variations in $\ln A$ occur with all parameters, but for higher frequencies the minima become very broad.

The qualitative interpretation of these results is

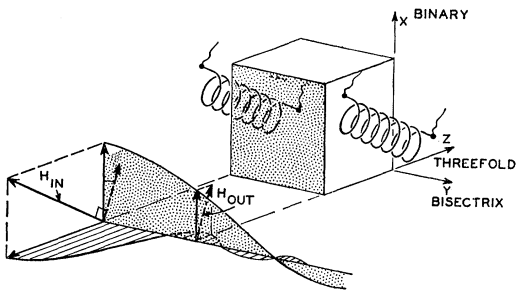

FIG. 11. Relationship of field vectors and crystallographic directions X, Y, and Z for producing a linearly polarized signal rotated by 90°, as explained in the text.

made with the aid of Fig. 11, which shows schematically the sample and a vector representation of the rf magnetic field. The input signal $\mathbf{H}_{\text{in}}$ is resolved along the binary and threefold directions. If we assume that a linearly polarized signal suffers no Hall effect rotation, these two signals will decay in the characteristic manner of damped Alfvén waves as shown by the instantaneous amplitudes. Since the wavelength of these waves is different for the two crystal directions, as we discussed before, the relative amplitudes at the output may be those shown in Fig. 11. It is clear from the figure that the signal in the output coil is zero because the rf field has rotated through 90°. When $\mathbf{H}_{\text{in}}$ is parallel to either the binary or threefold axes and the coils are parallel, an amount of transmission which is characteristic of that polarization direction is observed. From Fig. 9 (curve C), it is clear that these amounts are quite different for polarization along the binary or threefold axes. They are roughly in the ratio given by Buchsbaum[17] for the Alfvén velocities (~4 to 1) for a transmission path length of the order of one wavelength.

While no quantitative comparison with theory has been made, this interpretation appears to explain the observed effects. For example, with coils parallel, a null in the output can be expected only while the phase of output signal polarized along the threefold axis has reversed with respect to the input. The occurrence of the minima is, therefore, dependent on the wavelength and sample length. We interpret the disappearance of the sharp minima above 2 Mc/sec as resulting from the lack of phase reversal when the wavelength is between 3/4 and 5/4 times the sample length. Since at higher frequencies phase reversals can still occur in either the threefold or binary polarizations, this model can be expected to explain the high frequency dips shown in Fig. 4. The model particularly fits the results that the dips are only observed for transmission along the bisectrix axis, because only for this axis is there a significant difference in Alfvén velocity with polarization.[17]

VI. CONCLUSION

Low-frequency transmission of transverse hydromagnetic waves through sizable samples of Bi has been observed. The basic wave transmission characteristics, which are those of heavily damped waves, agree with those expected from a simple analysis of plane-polarized waves. Superimposed on this behavior, which is closely related to transverse magnetoresistance effects, is a rotation of the axis of polarization. The rotation results from the dependence of the wave properties on the direction of the transverse polarization with respect to the crystallographic axes, rather than a rotation caused by a residual Hall effect.

ACKNOWLEDGMENTS

The authors are indebted to S. J. Buchsbaum, A. G. Chynoweth, and J. K. Galt for a continuing interest in this work and to G. A. Baraff, S. J. Buchsbaum, and D. E. McCumber for a critical reading of the manuscript.

APPENDIX: ROTATION OF AXIS OF POLARIZATION WITH AND WITHOUT A DRIFT CURRENT

When a current is applied to the plasma, the dielectric constant $\epsilon_\pm$ in Eq. (7) contains a term which is linearly proportional to $k_\pm$. This term stems from the Doppler factor $(1-k_\pm V_d/\omega)$ acting on the Hall terms of the electrons and holes (V_d is the drift velocity).[12] For the present discussion, we note only that this term, like the $\pm\delta n/n$ term, has the opposite sign for the two polarizations and, therefore, causes a rotation. We assume a general form of Eq. (7)

$$k_\pm^2 = k_0 k_\pm \epsilon_{j\pm} + k_0^2(\epsilon_{r\pm} + i\epsilon_i), \tag{A1}$$

where $k_0=\omega/c$ and $\epsilon_{r\pm}$ and $\epsilon_{j\pm}$ are the Hall effect contributions of the $\pm\delta n/n$ and Doppler terms, respectively. The damped Alfvén-wave properties described earlier stem from the term ϵ_i, which is assumed to remain much larger in magnitude than either of the other terms. If either term were to be large, lightly damped waves of a helicon nature would propagate.

The signal amplitude, $A(\equiv A_x+iA_y$, where x is the direction of the source polarization and the wave, as before, propagates along z), is given by the sum of two circularly polarized components with propagation constants β_+ and β_- and attenuation coefficients α_+ and α_-

$$A=(A_0/2)\{\exp[i(\omega t-\beta_+ z)-\alpha_+ z] + \exp[-i(\omega t-\beta_- z)-\alpha_- z]\} \tag{A2}$$

$$=A_0 e^{-\bar{\alpha}z}[(\cos^2\delta\beta z+\sinh^2\delta\alpha z)^{1/2}\cos(\omega t-\bar{\beta}z-\psi_1) + i(\sin^2\delta\beta z+\sinh^2\delta\alpha z)^{1/2}\cos(\omega t-\bar{\beta}z-\psi_2)], \tag{A3}$$

where

$$2\bar{\beta}=\beta_++\beta_-;\quad 2\bar{\alpha}=\alpha_++\alpha_-,\qquad 2\delta\beta=\beta_+-\beta_-;\quad 2\delta\alpha=\alpha_+-\alpha_-, \tag{A4}$$

and

$$\tan\psi_1=\tan(\delta\beta z)\tanh(\delta\alpha z),\qquad \tan\psi_2=\cos(\delta\beta z)\tanh(\delta\alpha z). \tag{A5}$$

We see from the magnitudes of the real and imaginary

parts of Eq. (A3) that rotation of the axis of polarization is produced by nonzero $\delta\beta z$, while the ellipticity is described by $\delta\alpha z$. The first-order expressions for $\delta\beta$ and $\delta\alpha$ derived from Eq. (A1), assuming $\epsilon_i \gg \epsilon_r$, ϵ_j, are

$$|\delta\beta| = k_0\epsilon_j/2 + k_0\epsilon_r/(8\epsilon_i)^{1/2}, \quad \text{(A6)}$$

$$|\delta\alpha| = k_0\epsilon_r/(8\epsilon_i)^{1/2}, \quad \text{(A7)}$$

where we assumed $\bar{\beta}/(\bar{\beta}^2+\bar{\alpha}^2) \cong \bar{\alpha}/(\bar{\beta}^2+\bar{\alpha}^2) \cong (k_0{}^2 8\epsilon_i)^{-1/2}$. Equation (A6) shows that both Hall terms cause a rotation but from Eq. (A7) we see that to first order only the ϵ_r term gives rise to ellipticity. The amount of this ellipticity is, moreover, comparable in magnitude to the rotation as evidenced by the equal magnitudes of $\delta\beta$ and $\delta\alpha$.

PHYSICAL REVIEW VOLUME 152, NUMBER 2 9 DECEMBER 1966

Exchange Coupling and Conduction-Electron Polarization in Metals

R. E. WATSON
Brookhaven National Laboratory, Upton, New York*
and
Bell Telephone Laboratories, Murray Hill, New Jersey

AND

A. J. FREEMAN
National Magnet Laboratory,† Massachusetts Institute of Technology, Cambridge, Massachusetts

(Received 29 June 1966)

The exchange-coupling integral, $J(\mathbf{k},\mathbf{k}')$, between localized magnetic electrons and conduction electrons, treated as orthogonalized plane waves is investigated quantitatively for the case of a local moment which consists of the half-filled $4f^7$ shell of Gd^{3+} and for a range of $\mathbf{k}$ and $\mathbf{k}'$ values (the incident and scattered conduction-electron wave vectors). Ruderman-Kittel-Kasuya-Yosida (RKKY) theory is then employed, with and without an exchange-enhanced susceptibility, to obtain conduction-electron spin densities. For the special case of the rare-earth local moment, $J(\mathbf{k}, \mathbf{k}')$ is found to be well approximated by $J(Q)$ [where $Q \equiv |\mathbf{k}\text{-}\mathbf{k}'|$] but with a Q dependence which differs markedly from those traditionally assumed in RKKY theory. This severely affects spin-density predictions for a region extending several lattice sites away from the local-moment site. Use of the computed exchange coupling reduces the qualitative disagreement between theory and experiment.

I. INTRODUCTION

THE magnetic polarization of conduction electrons in alloys, pure metals, and intermetallic compounds containing local electronic magnetic moments, has been the object of extensive experimental investigation in recent years. Basic to the understanding of these observations is the familiar Ruderman-Kittel-Kasuya-Yosida (RKKY) theory[1] which in its original analytic form necessarily involved a number of important approximations. Since significant quantitative deviations have emerged between the predictions of the theory and experiment, questions concerning the validity of the approximations have been raised. In general, the susceptibility function has been considered to be chiefly responsible for these deviations and so attention has largely concentrated on this aspect of the theory.[2–4]

In this paper we inspect in detail the nature of the exchange coupling[5] between the local moment and the conduction electrons, i.e., the source of the conduction-electron polarization. The differences between the exact behavior of the coupling and that commonly assumed in the "simple" traditional theory will be seen to be as important for understanding the deviations between theory and experiment as are any refinements in the susceptibility. Indeed, an exact treatment of the exchange coupling *requires* abandonment of the utilization of the susceptibility function as used in the simple theory, a matter which will be inspected in a subsequent paper. A sampling of the exchange coupling will be made so that contact can be made with the traditional theory, Spin-density results will be reported for sus-

* Work supported by the U. S. Atomic Energy Commission.
† Work supported by the U. S. Air Force Office of Scientific Research.

[1] S. Vonsovskii, Zh. Eksperim. i Teor. Fiz. **16**, 981 (1946); **24**, 419 (1953); M. A. Ruderman and C. Kittel, Phys. Rev. **96**, 99 (1954); T. Kasuya, Progr. Theoret. Phys. (Kyoto) **16**, 45 (1965); A. H. Mitchell, Phys. Rev. **105**, 1439 (1957), and K. Yosida, *ibid.* **106**, 893 (1957). This list does not exhaust the early pertinent papers on the subject. The term "RKKY theory" represents a compromise with conventional usage.

[2] B. Giovannini, M. Peter, and J. R. Schrieffer, Phys. Rev. Letters **12**, 736 (1964).

[3] A. W. Overhauser and M. B. Stearns, Phys. Rev. Letters **13**, 316 (1964); the experiments relied on appear in M. B. Stearns and S. S. Wilson, Phys. Rev. Letters **13**, 313 (1964).

[4] T. Moriya, Progr. Theoret. Phys. (Kyoto) **34**, 329 (1965).

[5] A preliminary account appeared in R. E. Watson and A. J. Freeman, Phys. Rev. Letters **14**, 695 (1965).